Computational modelling and analysis of brain metabolism in neurodegenerative diseases

Supandi, F.B.

2016

document version
Publisher's PDF, also known as Version of record

Chapter 5

Computational prediction of changes in brain metabolic fluxes from mRNA expression in Alzheimer's disease

Farahaniza Supandi
Johannes HGM van Beek

Manuscript in preparation

Abstract

Alzheimer's disease (AD) is the most widespread neurodegenerative disorder. Studies have linked metabolic impairment, particularly glucose hypometabolism and mitochondrial dysfunction, with AD pathology. Although decreases in cerebral glucose and oxygen uptake have been measured in AD patients, little is known about the internal changes in the network of energy metabolism. Here we used an algorithm termed Lsei-FBA, which predicts how the metabolic flux distribution in central carbon metabolism is affected during the disease process. This makes use of measurements of gene expression in brain tissue of AD patients. We predict a decrease in glycolytic rate and oxygen consumption from the gene expression measurements that is in line with the experimental measurements (reductions of the order of 25%). The analysis predicts that ATP synthesis is reduced more strongly, by about 50%. A reduction is predicted for reaction fluxes in the first section of the TCA cycle, and a stronger reduction downstream of alpha-ketoglutarate. The latter reduction is partially compensated by upregulation of the GABA shunt. The transport of reducing equivalents from cytosol into mitochondria via the malate-aspartate shuttle is predicted to be substantially reduced, accompanied by a small increase in lactate production, but with little upregulation of the glycerol phosphate shuttle. We also found that changes in metabolic fluxes can be associated with specific brain regions: changes in the middle temporal gyrus, the hippocampus, posterior cingulate cortex and entorhinal cortex are large, while changes in the frontal gyrus and primary visual cortex remain smaller. We propose that the calculation of detailed metabolic flux changes from gene expression changes in diseased tissue may result in useful predictions.

Introduction

Alzheimer's disease (AD) is a type of neurodegenerative disease, which causes the most common type of dementia among the elderly worldwide. AD neuropathology is characterized by accumulation of extra-cellular β-amyloid (Aβ) plaques and intra-cellular neurofibrillary tangles (NFT), the latter caused by hyperphosphorylation of tau protein (Hardy & Selkoe 2002; Braak & Braak 1991). The precise etiologies and pathogenesis of AD still need to be understood. The amyloid cascade hypothesis has stimulated AD research in past decades, but recently it has been argued that this hypothesis should be rejected (Herrup 2015). Several alternative hypotheses may be considered. Some of these hypotheses involve impairment of energy metabolism. A loss of mitochondrial function may precede Alzheimer pathology and is the basis for the 'mitochondrial cascade hypothesis' for AD (Swerdlow et al. 2014). Glucose hypometabolism in the brain may also precede pathological signs of AD, even by many years, and deteriorating glucose metabolism has been proposed to contribute to the development of AD.

Although measurements of brain metabolic rates for glucose and oxygen with positron emission tomography (PET) are common (Chen & Zhong 2013; Cunnane et al. 2011), little is known on the details of changes in the energy metabolic network as a whole. The expression of genes in brain tissue of people who died with AD has been measured for many brain regions in several studies. This included many genes which code for the enzymes for central energy metabolism. The goal of the present study is therefore to predict the distribution of fluxes in the metabolic network for energy metabolism in the brain from the available gene expression measurements. Although an attempt was made to predict changes in metabolic fluxes in AD based on a large model of brain metabolism (Lewis et al. 2010), this was based on capacity measurements for one enzyme. It therefore appears useful to investigate whether gene expression measured for many enzymes in the network can be applied to predict changes in metabolic fluxes. To this end we will apply a recently developed algorithm for the prediction of flux changes from measured changes in the expression of the genes (Gavai et al. 2015).

The reduction of brain cerebral metabolic rate of glucose (CMRglc) is more prominent in specific brain areas (Mosconi 2005). PET studies with ^{18}F-fluorodeoxyglucose (FDG) in AD have demonstrated reductions of CMRglc in the parieto-temporal cortex and posterior cingulate cortex. While the disease progresses, the frontal cortex becomes involved, while the cerebellum, striatum, basal ganglia and primary and sensorimotor cortices remain relatively unaffected (Mosconi 2005; Braak & Braak 1991). Gene expression measurements are also available for specific brain regions, allowing anatomically detailed predictions of metabolic changes.

Gene expression studies of AD have been reported for several regions that are differentially affected. Liang at al. (Liang et al. 2007; 2008) analysed six regions including entorhinal cortex (EC), hippocampus (HIP), medial temporal gyrus (MTG), posterior cingulate cortex (PCC), superior frontal gyrus (SFG) and primary visual cortex (VCX). Berchtold at al. (Berchtold et al. 2013) analysed four regions including entorhinal cortex, hippocampus, post-central gyrus (PCG) and superior frontal gyrus. Blalock and his colleagues (Blalock et al. 2004; Blalock et al. 2011) analysed hippocampal gene expression of controls and patients across different levels of AD severity based on the Mini-Mental State Examination (MMSE) score and NFT. The last dataset we consider, by Dunkley at al. (Dunckley et al. 2006), is from the entorhinal cortex. Detailed statistical testing of these transcriptional datasets on the single gene level has already been discussed in the original publications. We do not repeat such statistical analysis but predict the change in flux distribution.

The Lsei-FBA approach is a recently proposed method to predict changes in metabolic network function based on gene expression measurement (Gavai et al. 2015). The assumption underlying this method is that, on average, fluxes catalysed by each enzyme tend to change to the same relative extent as expression of the genes coding for (subunits of) that enzyme. This assumption is not expected to be true at the level of each enzyme individually, but may be predictive when an entire network is considered. Because of the correlative approach which is not based on detailed and precise regulatory mechanisms and enzyme kinetic effects, it cannot be expected that this algorithm will yield very accurate predictions, but we propose that the algorithm may be useful to indicate direction and order of magnitude of changes in brain metabolism.

The Lsei-FBA approach has been discussed and tested in previous studies. The initial description of analysing flux distribution using this method was illustrated by applying it to one dataset from AD patients (Gavai et al. 2015). Lsei-FBA was also applied to a large number of datasets on Parkinson's disease (Chapter 4, this thesis). Here, we present an analysis involving more datasets for AD obtained for several distinct brain regions. The predicted changes in fluxes will be compared with measurements which are available for some fluxes, while predictions for several other unknown fluxes are derived.

Materials and methods

Datasets

The microarray data used in this study were obtained from the Gene Expression Omnibus (GEO) (Edgar et al. 2002) and are summarized in Supplementary Table 1. Datasets of Liang at al. and Dunkley at al. contained gene expression profiles from laser-captured microdissected neurons, while datasets from Berchtold at al. contains profiles

from whole tissue dissection of several brain regions that are known to be affected by the disease. Blalock at al., in their dataset of 2004 and 2011, compared stages of AD in different severity - incipient, moderate and severe. The first study uses whole tissue dissected from the CA1 hippocampal region, while the latter uses microdissected neurons of the same area. The gene expression was measured on Affymetrix chips (see Supplementary Table 1 for the type of chip). The Affymetrix CEL files were pre-processed and normalized using the RMA method (Irizarry et al. 2003). Log2 transformed values were used to calculate differences in expression levels of AD patients against healthy controls measured in the same laboratory on the same type of chip.

Metabolic network model of brain metabolism

The metabolic network model used in this study consists of the major pathways for central carbon metabolism. These pathways include glycolysis, pentose phosphate pathway (PPP), TCA cycle, oxidative phosphorylation (OxPhos), reducing equivalent shuttle mechanisms, glutamate-glutamine cycling, gamma-aminobutyric acid (GABA) shunt and transport of metabolites across the membranes which separate intracellular compartments. The selected reactions were imported from the reconstruction of human metabolism in the BiGG database (Schellenberger et al. 2010). A complete list of the reactions in the network, along with the list of metabolites are given in Supplementary Table 2 and 3. Supplementary Figure shows the network scheme. This model is the same as used in by Supandi & van Beek (Chapter 4, this thesis) and is discussed there in detail. We prefer to use this core model that has been accurately curated manually, rather than a 'genome-scale' model where each reaction has not been checked individually and which is often not free from errors.

Analysis of flux distribution

The method to analyse flux distribution in the healthy normal and diseased brain has been discussed in detail previously (Gavai et al., 2015; Chapter 4, this thesis). Here, we will discuss the method briefly. The metabolic system is assumed to be in (or very close to) steady state in the sense that changes in concentrations of metabolites inside the cell per unit time are negligible relative to the fluxes into and out of the metabolite pool. Substrate uptake and release measurements are used as constraints in the model. For the healthy elderly human brain (55-65 years), the uptake rates of glucose, and release of lactate, glutamine and pyruvate for the brain were reported to be 0.203, -0.0092, -0.011 and -0.0024 μmol g wet weight of brain^{-1} min^{-1} respectively (Lying-Tunell et al. 1980). A small flux which amounts to 6.9% of glycolysis is measured in the PPP in the normal brain (Dusick et al. 2007). Pyruvate carboxylation is 13% and glutamate-glutamine cycling fluxes is 62% of the value of the total glucose uptake in the brain (Hyder et al. 2006). The GABA shunt flux is 32% of the glucose uptake value (Patel et al.

2005). In the healthy brain, a cost function which maximizes ATP synthesis was assumed, as discussed extensively in (Gavai et al. 2015), The flux distribution was subsequently solved using the linear programming routine Linp from the package LIM (Soetaert & van Oevelen 2009) for the R programming environment.

For AD patients, the Lsei-FBA method is used to estimate the flux distribution, based on the changes in gene expression data and the flux distribution in normal brain calculated above (Gavai et al. 2015). For each reaction, the average fold change from controls was computed for the expression of each gene associated with the biochemical reactions in the model (Supplementary Table 4). If more than one gene-protein combination is associated with the enzyme reaction, the contribution is aggregated. An initial rough estimate of the flux for every reaction in the model is calculated by multiplying the fold change for gene expression in the AD patients and the flux estimated for the associated biochemical reaction for the healthy brain. Next, the flux estimate was refined based on flux balance in the model (Supplementary Figure).

Under the assumption of absolute flux balance of the internal metabolites in the model and of zero backflux for the irreversible reactions which are given in Supplementary Table 2, a cost function was minimized consisting of the sum of the squared deviations between final estimated flux and initial rough estimate of the flux as calculated above. This procedure was described in detail in Gavai et al. (2015) and Supandi & van Beek (Chapter 4, this thesis). The equations of this problem of least squares with equalities (balanced fluxes) and inequalities (irreversible reactions) were solved using the least squares with equality and inequality conditions (lsei) method from the limSolve package (Soetaert et al. 2009). This algorithm, termed Lsei-FBA, has already been described in detail in (Gavai et al. 2015).

Results

AD gene expression pattern across brain regions

For each reaction, the average fold changes of mRNA expression for patients with AD relative to healthy controls are shown in Supplementary Table 4 for various brain regions. Downregulated genes are shown in green, while upregulated genes are shown in red. Fold changes observed by Liang at al. are larger compared to the Berchtold at al. and Blalock at al. datasets, while in the dataset from Dunckley at al., changes in most reactions are small. In this respect the last dataset is an outlier.

Overall, fold changes for most of the reactions in the glycolytic pathway, TCA cycle, malate-aspartate shuttle and oxidative phosphorylation tend to show reduction of gene expression in all regions. Increased expression can be observed in nucleotide diphosphate kinase reaction (NDPK1m) and glutamine synthetase reaction (GLNS). The

glucose-6-phosphate dehydrogenase (G6PDH2r) and 6-phosphoglucolactonase (PGL) reactions at the entrance of the pentose phosphate pathway are also upregulated in most of the regions, with the entorhinal cortex in the Liang et al. dataset as conspicuous exception for all four enzymes. Please note that statistical analyses of the changes are found in the original publications on these datasets and are not repeated here.

Predicted flux distribution during Alzheimer's disease

We predict changes in metabolic fluxes distribution between the normal healthy brain and AD brain with the Lsei-FBA algorithm. The flux distribution for the normal brain has been predicted and discussed in (Gavai et al. 2015), and is given in Figure 1A. This distribution has also been compared extensively (Gavai et al. 2015) with the predicted flux distribution in a large model of brain metabolism (Lewis et al. 2010). Note that the oxygen uptake measured by (Lying-Tunell et al. 1980), 1.68 μmol g wet weight of brain^{-1} min^{-1}, is higher than predicted. When we had set the measured oxygen consumption as a constraint, the flux balance analysis did not yield a feasible solution, which reflects that the measured oxygen uptake is higher than can be accounted for by the carbon substrates taken up by the brain.

Comparison of flux prediction in all datasets for AD shows a pattern of reduction in the glucose and oxygen uptake, glycolytic pathway, TCA cycle and oxidative phosphorylation, while increases in flux are predicted for the PPP pathway, malic enzyme (ME) and pyruvate carboxylase (PC) reaction. In the Liang et al. dataset for different brain regions, glycolytic flux is predicted to be reduced 28.1% in HIP, 28% in EC, 26.9% in PCC, 25.7% in MTG, 13.8% in VCX and 10.7% in SFG. ATP synthesis in the mitochondria is predicted to be reduced by 51.7% in PCC, 43.5% in HIP, 39% in MTG, 26.8% in VCX, 25.7% in EC and 17.6% in SFG. Oxygen uptake is predicted to be reduced 51.4% in PCC, 42.8% in HIP, 38.4% in MTG, 26.6% in VCX, 25.2% in EC and 17.5% in SFG (Supplementary Table 5). Note that the relative reduction in oxygen consumption and ATP synthesis is in several cases substantially larger than the reduction in glucose uptake. Figure 1B - 1D shows fluxes predicted based on the Liang at al. dataset. Figure 1B and 1C shows predicted flux distributions during AD in the hippocampus and posterior cingulate cortex, respectively. Figure 1D shows the flux distribution in the SFG, the region which showed the smallest flux declines in the Liang at al. study.

Smaller changes were found for predicted fluxes across brain regions in the Berchtold at al. dataset. Glycolytic pathway fluxes were reduced by about 10.7% (EC) to 6.8% (PCG), ATP synthesis was reduced by about 14.4% (HIP) to 7.9% (PCG), oxygen uptake reduced by about 14% (HIP) to 7.7% (PCG).

According to the prediction, fluxes in the pentose phosphate pathway (PPP) are increased in most of the regions ranging from 18% to 155% increase. No consistent increase or decrease in flux is found in the glutamine-glutamate cycle and the GABA shunt. The substantial predicted changes in flux for malic enzyme (ME2m) and pyruvate

carboxylase (PCm) in the mitochondria are noteworthy. These two enzymes potentially form a bypass of MDHm; however, this result needs to be interpreted with care (see Discussion). The glycerol phosphate shuttle to transport reducing equivalents from the cytosol into the mitochondria is predicted to be slightly activated for some data sets. Predicted fluxes in the malate-aspartate shuttle are consistently, although moderately, decreased.

In many of the datasets the relative reduction in the AKDGm reaction is predicted to be considerably stronger than in the section between citrate and alpha-ketoglutarate which precedes it in the TCA cycle. This is compensated to a small degree by an increase in the GABA shunt flux. A considerable decrease in alpha-ketoglutarate production from glutamate via aspartate transaminase is also predicted. However, this decrease is exactly balanced by the change in alpha-ketoglutarate export from the mitochondria in exchange for malate which is part of the malate-aspartate shuttle. If we look at the HIP dataset of Liang (Supplementary Table 5) as an example, we see that the decrease in alpha-ketoglutarate (AKG) uptake by the AKGDm reaction is 0.169 μmol g wet weight of brain^{-1} min^{-1} which is balanced by a 0.097 μmol g ww^{-1} min^{-1} decrease in AKG production by the ICDHxm reaction, a 0.028 larger uptake by the GLUDym reaction and a 0.045 larger uptake by the ABTArm reaction.

Comparisons across stages of the disease with different severity can be made based on the Blalock at al. datasets for the hippocampal region. The flux predictions show larger changes in fluxes during the more severe stage of the disease, except for the severe stage in the Blalock at al. 2011 dataset measured in excised neurons rather than whole tissue, where the fluxes are relatively unchanged. In the Blalock 2004 at al. dataset, fluxes in glycolytic pathway are reduced by 8.7% (MOD) and 19% (SEV), ATP synthesis is reduced by 19.6% (MOD) and 31.4% (SEV), and oxygen uptake is reduced by 19.4% (MOD) and 31% (SEV).

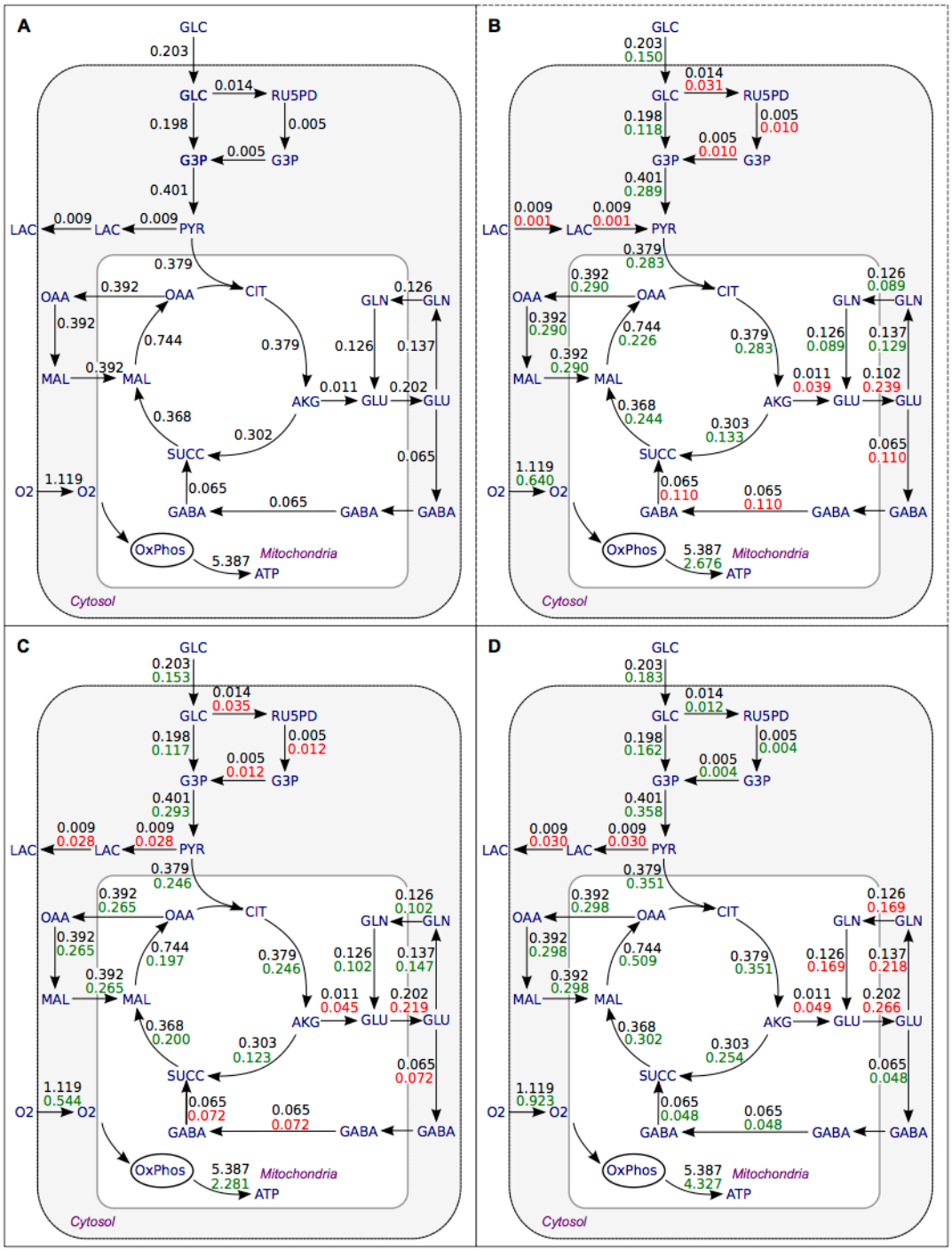

Figure 1. Flux distribution in healthy brain and during Alzheimer's disease.

Flux distribution in healthy brain (A) and during AD from the Liang et al. dataset in hippocampal region (B), posterior cingulate cortex (C) and superior frontal gyrus (D) in µmol g (wet) brain^{-1} min^{-1}. Black numbers, flux during normal condition; green numbers, flux decreased during AD and red numbers, increased from the normal condition. Note that for clarity not all separate biochemical steps are plotted: oxaloacetate is for instance first transaminated to aspartate before being transported across the mitochondrial membrane as part of the malate-aspartate shuttle. GLC, glucose; G3P, glyceraldehyde 3-phosphate; RU5PD, ribulose-5-phosphate; PYR, pyruvate; LAC, lactate; CIT, citrate; AKG, alpha-ketoglutarate; SUCC, succinate; MAL, malate; OAA, oxaloacetate; GLU, glutamate; GLN, glutamine, GABA, 4-aminobutanoate

(synonym of gamma-aminobutyrate); O2, oxygen; OxPhos, oxidative phosphorylation. Flux values from GLC to RU5PD and from RU5PD to G3P represent 6-carbon units leaving the GLC pool rather than 3-carbon units entering the G3P pool.

Discussion

Brain energy metabolism and Alzheimer's disease

Under normal physiological conditions the brain relies almost exclusively on glucose as its main substrate for energy production. ATP is mostly produced in the mitochondria from the oxidation of glucose under aerobic conditions. Almost all of the glucose is oxidized to water and CO_2 (Clarke & Sokoloff 1999). Thus, glucose hypometabolism can severely affect brain energy supply. Alternative substrates other than glucose may be used under certain circumstances. Glycogen provides an emergency store of carbohydrates, but there is a limited amount (Clarke & Sokoloff 1999) which has to be restored from glucose. Ketone bodies, in the form of acetoacetate and β–hydroxybutyrate, may replace glucose to a large extent during extended fasting or starvation. Compared to the substantial decrease in glucose uptake, brain ketone uptake is not significantly affected during aging or AD (Lying-Tunell et al. 1981; Castellano et al. 2015). Nevertheless, supplying ketone bodies has been proposed as a therapeutic measure during AD (Cunnane et al. 2011).

Brain energy metabolism is supported by three major processes - cerebral blood flow, oxygen consumption and glucose metabolism (Cunnane et al. 2011). All of these can be measured, among others with positron emission tomography (PET). Decreases in cerebral metabolic rate (CMR) for glucose (Minoshima et al. 1997; Li et al. 2008; Mosconi 2005; Mosconi et al. 2008; Cunnane et al. 2011) and oxygen (Ishii et al. 1996) have been reported in AD. The decrease in metabolic rate in the temporal lobe measured by positron emission tomography (PET) was 23% for oxygen (Ishii et al. 1996) and 36% for glucose (Ishii et al. 1997). Supplementary Table 6 gives an overview of available measurements and a comparison with the present predictions from gene expression. The global cerebral metabolic rate for glucose (CMRglc) is reduced by 20 – 25% in AD (reviewed in Cunnane et al. 2011). The direction and order of magnitude of flux changes predicted in the present study agrees with measured glucose and oxygen uptake rates measured experimentally.

Decrease in cerebral glucose metabolism and severity of AD pathology both differ across brain regions (Mosconi 2005). The most vulnerable areas during AD are the medial temporal lobe, entorhinal and perirhinal cortex, and hippocampus (Mosconi 2013). When compared with age-matched controls, AD individuals show metabolic reductions in regional glucose metabolism in posterior cingulate cortex during disease progression (~21% compared to our prediction of 25%, Supplementary Table 6)

(Minoshima et al. 1997). In contrast, the primary motor and visual cortex, cerebellum and basal ganglia nuclei are less severely affected (Mosconi 2005). This is also seen in our prediction from the Liang at al. dataset, where flux changes are larger in PCC, EC, HIP and MTG, while SFG and VCX show smaller changes (See Supplementary Table 5 and 6).

There is evidence that Aβ can have a severe detrimental effect on mitochondrial function through several pathways, such as impairment of oxidative phosphorylation, elevation of reactive oxygen species production, alteration of mitochondrial dynamics and interaction with mitochondrial proteins. This may subsequently leads to loss of synaptic function and neuronal cell death (reviewed in Eckert et al. 2011). It is not yet clear whether decrease in function leads to decrease of metabolism or the other way around.

As a consequence of reduced glucose metabolism, a decrease in ATP production has been estimated, which tends to increase during the course of the disease, by up to 50% in advanced AD (Hoyer 1992). This is similar to our present predictions. Analysis from mRNA gene expression data (Liang et al. 2008) with our algorithm leads to the prediction that energy metabolism in the brain is strongly compromised, particularly affecting reactions in the mitochondria. Some key enzymes in the citric acid cycle pathway - pyruvate dehydrogenase (PDHm), cytochrome oxidase (CYOOm3) and alpha ketoglutarate dehydrogenase (AKGDHm) are reduced during AD (Blass 2001; Chandrasekaran et al. 1994). A decrease in AKGDm activity has been found by biochemical assay (Bubber et al. 2005). Based on a 57% decrease in AKGDm activity, a substantial decrease in metabolic rates in glutamatergic and cholinergic neurons was predicted in an analysis with a large model of brain metabolism, but metabolic rates were maintained in GABAergic neurons where the GABA shunt pathway was activated to compensate for reduced AKGDm activity (Lewis et al. 2010). Here we predict metabolic flux changes for brain tissue based on gene expression distributed across the whole metabolic network. The predictions from the model of Lewis et al. (2010) and our present analysis underline mitochondrial dysfunction in AD.

Our model prediction is that lactate transport out of the brain is increased in many brain regions, while increases in lactate and pyruvate levels have been measured in the cerebrospinal fluid of AD patients (Liguori et al. 2014; Redjems-Bennani et al. 1998). However, for many brain regions an increased uptake of pyruvate is predicted in our present analysis. In general similar trends in metabolism in AD patients are seen in calculated predictions and independent measurements for glucose and oxygen metabolism.

While glucose and oxygen uptake and lactate and pyruvate levels have been measured in AD and comparisons with predicted fluxes for these metabolites are possible, the present analysis provides further predictions for fluxes internal to the metabolic network that have not yet been measured. Given the qualitative

correspondence between predictions and measurements where available, the model predictions for those parts of the metabolic network that are not yet accessible for measurements in patient studies may be of interest and can among others be used for further assessment of the validity of the model if these fluxes become measurable in the future.

The predictions suggest that malate-aspartate flux is substantially downregulated in many brain regions. This conforms with lower NADH production as a consequence of lower glycolytic activity, and is enhanced further by NADH used for lactate production. In contrast, the glycerol phosphate shuttle flux is somewhat upregulated in many regions.

The core model of brain energy metabolism used in the present study contains malic enzyme and pyruvate carboxylase. Acting in concert these enzymes can bypass the mitochondrial malate dehydrogenase. ME2m and PCm have been included in several models of brain energy metabolism (Calvetti & Somersalo 2013; Cakir et al. 2007; Occhipinti et al. 2010; Lewis et al. 2010). Both ME and PC occur in the brain according to biochemical measurements. As such these are added to the model. However, ME is neuronal, mitochondrial and NADP dependent, while PC is astrocytic and mitochondrial (Hassel 2001). These locations would suggest that the considerable increase in flux via both enzymes is coupled via pyruvate diffusion between neurons and astrocytes. Some flux is redistributed from neuronal MDHm to production of pyruvate, CO_2 and NADPH in the neuronal mitochondria. The decrease in NADH production by MDHm would lead to a reduction in predicted O_2 uptake and mitochondrial ATP production. In the astrocytes one ATP would then be consumed to synthesize oxaloacetate. The predicted effects of the loop formed by ME2m and PCm mean a decrease in predicted net mitochondrial ATP production, while NADPH is formed in the neuron (potentially useful for reactive oxygen species detoxification), and oxaloacetate is synthesized in the astrocyte, resulting in a special form of anaplerosis.

However, we emphasize that while the enzymes connected with ME2m and PCm are found in brain tissue, it is possible that regulatory processes prevent that this cycle is actually more active in brain tissue during AD. If this cycle is not upregulated in reality, this would mean that mitochondrial ATP production is underestimated by our present calculations. It is remarkable that the predicted flux via ME2m and PCm is increased despite a decrease in mRNA expression levels which is found in most cases. This is the consequence of the substantial reduction in MDHm expression which is greater than the reduction of ME2m and PCm expression.

There is a strong relationship of brain hypometabolism and AD. The question arises whether deteriorating brain metabolism causes AD or vice versa. Brain hypometabolism may be caused by impairment of glucose uptake and/or downstream steps of glucose utilization and may even causally contribute to the development of AD neuropathology (Cunnane et al. 2011; Mosconi 2013). This may involve

neurodegeneration and accumulation of Aβ plaques, developing the clinical symptoms of AD i.e. memory loss and behavioural change. Such changes in brain function may in turn affect ATP consumption and synthesis. The reason that brain hypometabolism is considered an upstream event during AD development is because it is known to be altered at very early stages (Cunnane et al. 2011). Moreover, whether hypometabolism in brain specifically affects only glucose metabolism alone or also other brain energy sources such as ketone bodies as glucose replacement are not yet resolved (Cunnane et al. 2011; Eckert et al. 2011).

Gene expression changes differ when comparing datasets from measurements of a whole tissue and dissected neurons (Supplementary Table 5). Flux changes in the Liang at al. dataset on neurons tend to show larger changes as compared to the Berchtold at al. dataset for whole brain tissue. Stempler at al. concluded that metabolic genes show higher accuracy for predicting AD progression and cognitive decline from hippocampal gene expression in dissected neurons than for whole tissue (Stempler et al. 2012). However, gene expression changes are less consistent when comparing the 2004 whole tissue dataset and the 2011 microdissected neuron dataset of Blalock et al. (Blalock et al. 2004; Blalock et al. 2011).

Limitations of this study

Of course there are several important limitations to this study. The concept that at the level of a metabolic network fluxes tend to change proportionally to the expression of the associated metabolic genes has been tested only on brain tissue from Alzheimer and Parkinson's disease patients. Nevertheless, gene expression levels have been shown to give good predictions of flux distribution in yeast (Lee et al. 2012). Other proposed algorithms to predict metabolic flux from gene expression (changes) are less well suited for the present situation where many genes are altered relatively modestly in expression (Gavai et al. 2015). The results for PD and AD look promising, although relatively few flux measurements were available for comparison.

Our model does only include the core of energy metabolism. These reactions are also connected with the broader metabolic network represented by genome-scale reconstructions of metabolism. However, comparison (Gavai et al. 2015) of results from the present model with a large model of brain metabolism (Lewis et al. 2010) suggested that the omitted connections to broader metabolism carry negligible fluxes.

Our model does not take into account the compartmentation of brain metabolism in several cell types, such as neurons, glia and endothelium. This was inspired by the nature of the data where gene expression has not been differentiated between the cell types. As illustrated by the example of the different locations of ME2m and PCm (see above) this may have consequences for the outcome. The present analysis therefore incorporates the assumption that changes in transport processes between the various cell types do not have a large effect on the metabolic system.

Conclusion

In this study, we describe the application of a recently developed algorithm to predict changes in metabolic fluxes based on gene expression changes from Alzheimer's disease patients. Fluxes through central carbon metabolism are predicted to be reduced in most regions. This reduction differs across regions and to some extent parallels differences in AD pathology. Reduced metabolism via alpha ketoglutarate dehydrogenase in the middle of the TCA cycle is partially compensated via the GABA shunt. Changes in metabolic fluxes are associated with specific regional pattern: changes in the middle temporal gyrus and the hippocampus, posterior cingulate cortex and entorhinal cortex are larger while changes the frontal gyrus and primary visual cortex remains minimum. This parallels the severity of AD pathology.

Supplementary materials

Supplementary Table 1 – Supplementary of all datasets used in this study
Supplementary Table 2 – List of reactions included in this model after extraction from the Recon1 knowledgebase for human metabolism
Supplementary Table 3 – List of metabolites included in this model, extracted from the Recon 1 knowledgebase
Supplementary Table 4 – Average fold changes of gene expression for each reaction
Supplementary Table 5 – Results for flux prediction for Alzheimer's disease datasets
Supplementary Table 6 – Predicted flux in this study (between parentheses) compared to experimental results in Alzheimer's disease
Supplementary Figure – Reconstructed metabolic reaction network

References

Berchtold, N.C. et al., 2013. Synaptic genes are extensively downregualted across multiple brain regions in normal human aging and Alzheimer's disease. *Neurobiology of Aging*, 34(6), pp.1653–1661.

Blalock, E.M. et al., 2004. Incipient Alzheimer's disease: microarray correlation analyses reveal major transcriptional and tumor suppressor responses. *Proceedings of the National Academy of Sciences of the United States of America*, 101(7), pp.2173–2178.

Blalock, E.M. et al., 2011. Microarray analyses of laser-captured hippocampus reveal distinct gray and white matter signatures associated with incipient Alzheimer's disease. *Journal of Chemical Neuroanatomy*, 42(2), pp.118–126.

Blass, J.P., 2001. Brain metabolism and brain disease: Is metabolic deficiency the proximate cause of Alzheimer dementia? *Journal of Neuroscience Research*, 66(5),

pp.851–856.

Braak, H. & Braak, E., 1991. Neuropathological stageing of Alzheimer-related changes. *Acta Neuropathologica*, 82(4), pp.239–259.

Bubber, P. et al., 2005. Mitochondrial abnormalities in Alzheimer brain: Mechanistic implications. *Annals of Neurology*, 57(5), pp.695–703.

Cakir, T. et al., 2007. Reconstruction and flux analysis of coupling between metabolic pathways of astrocytes and neurons: application to cerebral hypoxia. *Theoretical Biology & Medical Modelling*, 4, p.48.

Calvetti, D. & Somersalo, E., 2013. Quantitative in silico Analysis of Neurotransmitter Pathways Under Steady State Conditions. *Frontiers in Endocrinology*, 4, p.137.

Castellano, C.A. et al., 2015. Lower brain 18F-fluorodeoxyglucose uptake but normal 11C-acetoacetate metabolism in mild Alzheimer's disease dementia. *Journal of Alzheimer's Disease*, 43(4), pp.1343–1353.

Chandrasekaran, K. et al., 1994. Impairment in mitochondrial cytochrome oxidase gene expression in Alzheimer disease. *Molecular Brain Research*, 24(1-4), pp.336–340.

Chen, Z. & Zhong, C., 2013. Decoding Alzheimer's disease from perturbed cerebral glucose metabolism: Implications for diagnostic and therapeutic strategies. *Progress in Neurobiology*, 108, pp.21–43.

Clarke, D. & Sokoloff, L., 1999. Circulation and Energy Metabolism of the Brain. In G. Siegel et al., eds. *Basic Neurochemistry: Molecular, Cellular and Medical Aspects.* New York: Raven Press, pp. 637–669.

Cunnane, S. et al., 2011. Brain fuel metabolism, aging, and Alzheimer's disease. *Nutrition*, 27, pp.3–20.

Dunckley, T. et al., 2006. Gene expression correlates of neurofibrillary tangles in Alzheimer's disease. *Neurobiology of Aging*, 27(10), pp.1359–1371.

Dusick, J.R. et al., 2007. Increased pentose phosphate pathway flux after clinical traumatic brain injury: a [1,2-13C2]glucose labeling study in humans. *Journal of Cerebral Blood Flow and Metabolism*, 27(9), pp.1593–1602.

Eckert, A., Schmitt, K. & Götz, J., 2011. Mitochondrial dysfunction - the beginning of the end in Alzheimer's disease? Separate and synergistic modes of tau and amyloid-β toxicity. *Alzheimer's Research and Therapy*, 3(2), p.15.

Edgar, R., Domrachev, M. & Lash, A.E., 2002. Gene Expression Omnibus: NCBI gene expression and hybridization array data repository. *Nucleic Acids Research*, 30(1), pp.207–210.

Gavai, A.K. et al., 2015. Using Bioconductor package BiGGR for metabolic flux estimation based on gene expression changes in brain. *PLoS ONE*, 10(3), p.e0119016.

Hardy, J. & Selkoe, D.J., 2002. The amyloid hypothesis of Alzheimer's disease: progress and problems on the road to therapeutics. *Science*, 297(5580), pp.353–356.

Hassel, B., 2001. Pyruvate carboxylation in neurons. *Journal of Neuroscience Research*, 66, pp.755–762.

Herrup, K., 2015. The case for rejecting the amyloid cascade hypothesis. *Nature*

Neuroscience, 18(6), pp.794–799.

Hoyer, S., 1992. Oxidative energy metabolism in Alzheimer brain. Studies in early-onset and late-onset cases. *Molecular and Chemical Neuropathology*, 16, pp.207–224.

Hyder, F. et al., 2006. Neuronal-glial glucose oxidation and glutamatergic-GABAergic function. *Journal of Cerebral Blood Flow and Metabolism*, 26(7), pp.865–77.

Irizarry, R.A. et al., 2003. Exploration, normalization, and summaries of high density oligonucleotide array probe level data. *Biostatistics*, 4(2), pp.249–264.

Ishii, K. et al., 1996. Decreased medial temporal oxygen metabolism in Alzheimer's disease shown by PET. *Journal of Nuclear Medicine*, 37(7), pp.1159–1165.

Ishii, K. et al., 1997. Reduction of cerebellar glucose metabolism in advanced Alzheimer's disease. *Journal of Nuclear Medicine*, 38(6), pp.925–928.

Lee, D. et al., 2012. Improving metabolic flux predictions using absolute gene expression data. *BMC Systems Biology*, 6(1), p.73.

Lewis, N.E. et al., 2010. Large-scale in silico modeling of metabolic interactions between cell types in the human brain. *Nature Biotechnology*, 28(12), pp.1279–1285.

Li, Y. et al., 2008. Regional analysis of FDG and PIB-PET images in normal aging, mild cognitive impairment, and Alzheimer's disease. *European Journal of Nuclear Medicine and Molecular Imaging*, 35(12), pp.2169–2181.

Liang, W.S. et al., 2007. Gene expression profiles in anatomically and functionally distinct regions of the normal aged human brain. *Physiological Genomics*, 28(3), pp.311–322.

Liang, W.S. et al., 2008. Alzheimer's disease is associated with reduced expression of energy metabolism genes in posterior cingulate neurons. *Proceedings of the National Academy of Sciences of the United States of America*, 105(11), pp.4441–4446.

Liguori, C. et al., 2014. CSF lactate levels, τ proteins, cognitive decline: a dynamic relationship in Alzheimer's disease. *Journal of Neurology, Neurosurgery, and Psychiatry*.

Lying-Tunell, U. et al., 1980. Cerebral blood flow and metabolic rate of oxygen, glucose, lactate, pyruvate, ketone bodies and amino acids. *Acta Neurologica Scandinavica*, 62, pp.265–275.

Lying-Tunell, U. et al., 1981. Cerebral blood flow and metabolic rate of oxygen, glucose, lactate, pyruvate, ketone bodies and amino acids. *Acta Neurologica Scandinavica*, 63, pp.337–350.

Minoshima, S. et al., 1997. Metabolic reduction in the posterior cingulate cortex in very early Alzheimer's disease. *Annals of Neurology*, 42(1), pp.85–94.

Mosconi, L., 2005. Brain glucose metabolism in the early and specific diagnosis of Alzheimer's disease: FDG-PET studies in MCI and AD. *European Journal of Nuclear Medicine and Molecular Imaging*, 32(4), pp.486–510.

Mosconi, L., 2013. Glucose metabolism in normal aging and Alzheimer's disease: Methodological and physiological considerations for PET studies. *Clinical and*

Translational Imaging, 1, pp.217–233.

Mosconi, L., Pupi, A. & De Leon, M.J., 2008. Brain glucose hypometabolism and oxidative stress in preclinical Alzheimer's disease. *Annals of the New York Academy of Sciences*, 1147, pp.180–195.

Occhipinti, R., Somersalo, E. & Calvetti, D., 2010. Energetics of inhibition: insights with a computational model of the human GABAergic neuron-astrocyte cellular complex. *Journal of Cerebral Blood Flow and Metabolism*, 30(11), pp.1834–46.

Patel, A.B. et al., 2005. The contribution of GABA to glutamate/glutamine cycling and energy metabolism in the rat cortex in vivo. *Proceedings of the National Academy of Sciences of the United States of America*, 102(15), pp.5588–93.

Redjems-Bennani, N. et al., 1998. Abnormal substrate levels that depend upon mitochondrial function in cerebrospinal fluid from Alzheimer patients. *Gerontology*, 44, pp.300–304.

Schellenberger, J. et al., 2010. BiGG: a Biochemical Genetic and Genomic knowledgebase of large scale metabolic reconstructions. *BMC Bioinformatics*, 11, p.213.

Soetaert, K., van Den Meersche, K. & van Oevelen, D., 2009. limSolve: Solving linear inverse models.: R package version 1.5. Available at: http://lib.stat.cmu.edu/R/CRAN/web/packages/limSolve/index.html.

Soetaert, K. & van Oevelen, D., 2009. LIM: Linear inverse model examples and solution methods.: R package version 1.4. Available at: http://lib.stat.cmu.edu/R/CRAN/web/packages/LIM/index.html.

Stempler, S. et al., 2012. Hippocampus neuronal metabolic gene expression outperforms whole tissue data in accurately predicting Alzheimer's disease progression. *Neurobiology of Aging*, 33(9), pp.2230.e13–2230.e21.

Swerdlow, R.H., Burns, J.M. & Khan, S.M., 2014. The Alzheimer's disease mitochondrial cascade hypothesis: Progress and perspectives. *Biochimica et Biophysica Acta*, 1842(8), pp.1219–1231.